Molecular Biology Reports (2022) 49:4777–4793
https://doi.org/10.1007/s11033-022-07329-w

ORIGINAL ARTICLE

Proteasome inhibitor immunotherapy for the epithelial to mesenchymal transition: assessing the A549 lung cancer cell microenvironment and the role of M1, M2a and M2c 'hydrocortisone-polarised' macrophages

Selin Engür-Öztürk[1] · **Miriş Dikmen**[2]

Received: 15 November 2021 / Accepted: 2 March 2022 / Published online: 13 March 2022

Abstract

Background Lung cancer is a leading cause of cancer-related deaths, primarily as a result of metastases. In this metastasis, the epithelial-to-mesenchymal transition (EMT) is essential. Interaction with the cancer cell microenvironment is primarily dependent on M1- and M2-polarized macrophage.

Methods and results In this study, we revealed the EMT-associated activity of M1, M2a and M2c macrophages in A549 lung cancer cells. We established a co-culture model of A549 lung cancer cells utilizing THP-1-derived M1/M2 polarised macrophages to explore the involvement of macrophages in the immune response, apoptosis, and EMT in lung cancer. Although multiple polarising agents are routinely used for M1 and M2 conversion, we assessed a new possible polarising agent, hydrocortisone.

Conclusions M1 increased A549 cell sensitivity to proteasome inhibitors and decreased A549 cell viability by inducing apoptosis. EMT was induced in the presence of M2c macrophages in A549 cells by the levels of vimentin, fibronectin, E-cadherin, NF-kB, CCL-17. We also revealed the antiproliferative effects of bortezomib and ixazomib on A549 cells in both 2D and 3D cultures. Our findings could help develop an immunotherapeutic strategy by shedding light on a previously undiscovered part of the EMT pathway. Furthermore, additional investigation may reveal that polarising tumour-associated macrophages to M1 and eliminating the M2a or particularly the M2c subtype are effective anti-cancer strategies.

Keywords A549 · Macrophages · EMT · NF-kB · Bortezomib · Ixazomib

Introduction

Cancer is uncontrolled cell proliferation caused by genetic and epigenetic abnormalities. Cell death resistance, triggered angiogenesis, invasion, and metastasis are all hallmarks of cancer [1]. Lung cancer is the most frequently diagnosed type of cancer and the leading cause of cancer-related death globally [2]. Lung cancer deaths are mostly due to cancer progression during or after systemic therapy. Resistance to systemic treatments is therefore a major hurdle in treating non-small cell lung cancer. As a result, developing novel treatment approaches for patients with lung cancer may help to improve their prognosis [3].

The microenvironment defines non-cancer cells and tumor tissue structures, and an inflammatory microenvironment is a major factor in lung cancer progression. Tumor-Associated Macrophages (TAMs) are important members of the cancer microenvironment, and they have a variety of therapeutic effects on lung tumor progression [4]. Tumor-associated macrophages make up 5–40% of the tumor mass in solid tumors [5]. Macrophages are studied in two functionally distinct subgroups: pro-inflammatory (M1 macrophage) and anti-inflammatory (M2 macrophage) [6–8]. M1 macrophages can be polarized to the M1 phenotype in

✉ Selin Engür-Öztürk
selino@pau.edu.tr

Miriş Dikmen
mirisd@anadolu.edu.tr

[1] Department of Pharmacy Services, Tavas Health Services Vocational School, Pamukkale University, Tavas, 20500 Denizli, Turkey

[2] Department of Pharmacology, Faculty of Pharmacy, Anadolu University, Eskişehir, Turkey

the presence of interferon-gamma (IFN-γ) and inflammatory stimuli such as tumor necrosis factor-alpha (TNF-alpha) or lipopolysaccharide (LPS) [9, 10]. M2 macrophages are polarized to M2a, M2b, and M2c macrophages with different stimuli. M2a polarization occurs in the presence of Interleukin-4 (IL-4) and Interleukin-13 (IL-13). M2c macrophages are polarized by the presence of glucocorticoids, Transforming Growth Factor Beta (TGF-β) or Interleukin-10 (IL-10) [11]. In this study, we used hydrocortisone 'well-known glucocorticoid' for the first time in M2c polarization, especially focusing more on M2c macrophages. M1 and M2 tumor-associated macrophages are central in the relationship between chronic inflammation conditions in cancer [12, 13] and play a vital role in the growth of tumors, EMT, angiogenesis, cancer metastases, and drug resistance [13].

EMT is a morphological transformation of cells from an epithelial-polarized phenotype to a mesenchymal fibroblastoid phenotype that plays a critical role in cancer metastasis [14]. In the development process, a balanced epithelial-mesenchymal transition is essential, while abnormal EMT contributes to pathogenesis by disrupting epithelial homeostasis for diseases such as cancer [15]. NF-kB (nuclear factor kappa B) is a key marker for cancer invasion and EMT [16, 17]. NF-kB is a transcription factor that regulates gene-encoding molecules such as chemokines, apoptosis, surface receptors in the immune response, cytokines, cell adhesion molecules, and inflammation [18].

Proteasome inhibitors have a wide range of molecular effects, including inhibition of NF-kB, and the conventional wisdom is that they block the activation of NF-kB and the degradation of other proteins, resulting in cytotoxicity in sensitive cell types [19]. The first proteasome inhibitor, bortezomib (Velcade), was approved by the US Food and Drug Administration (FDA), and ixazomib (Ninlaro) was recently approved [19–21]. Numerous studies have discovered evidence for decreased nuclear factor (NF)-kB activation as a result of bortezomib mediated stabilization of the inhibitor IkB [19, 22]. Proteasome inhibitors in combination with conventional anticancer agents and novel immunotherapy approaches are demonstrating great promise [19]. Several therapeutic approaches have been proposed in recent years, focusing on the NF-kB axis targeting tumour invasion. We utilised 2D and 3D cell culture approaches to evaluate the effects of bortezomib and ixazomib, recently developed therapeutic strategies, on antiproliferative, apoptotic and EMT pathways in A549 lung cancer co-cultures that included THP-1-derived M1, M2a and M2c polarised macrophages. This is the first article of M2c macrophage polarization by hydrocortisone that we are aware of.

Materials and methods

Chemicals

Hydrocortisone, Eagle's Minimum Essential Medium (EMEM), phorbol 12-myristate 13-acetate (PMA), phosphate-buffered saline (PBS), RPMI-1640 medium, bovine serum albumin (BSA), interleukin-4 (IL-4), dimethyl sulfoxide (DMSO), fetal bovine serum (FBS), lipopolysaccharide (LPS), interferon-γ (IFN-γ), hoechst 33258 dye and interleukin-13 (IL-13) were purchased from Sigma Aldrich (St. Louis, MO, USA). Vimentin monoclonal antibody (vimentin [D21H3] XP® Rabbit mAb) and secondary anti-rabbit Alexa Fluor 594 (anti-rabbit IgG [H + L], F(ab') 2 fragment [Alexa Fluor® 594 Conjugate]), e-cadherin monoclonal antibody (E-cadherin [4A2] mouse mAb) and secondary antibody anti-mouse Alexa Fluor 488 (ab150113, Abcam) were purchased from Cell Signaling (Danvers, MA, USA).

Cell culture and treatments

Non-small cell lung cancer cells A549 (CCL-185, ATCC®, USA), human lung fibroblast cells CCD-19Lu (CCL-210, ATCC®, USA), and human monocyte cells THP-1 (TIB-202, ATCC®, USA) were cultured in RPMI-1640 medium with 1% penicillin–streptomycin and 10% FBS (Sigma; St. Louis, MO, USA). Cultures were incubated at 37 °C in a humidified CO_2 (5%) incubator (Heracell™, Thermo Fisher Scientific™, Pittsburgh, PA, USA). Bortezomib (BioChemica, Sauerlach, Germany) and ixazomib (Active Biochem, Germany) were dissolved in DMSO. The control group was incubated in a 0.1 percent DMSO-containing medium.

Polarisation of macrophages into M1, M2a, and M2c subtypes

THP-1 cells were treated with 100 ng/mL PMA in serum-free medium (SFM) for 24 h to induce differentiation into a macrophage-like phenotype. To obtain the macrophage (M0) resting state, differentiated adherent cells were rested in the culture medium (without the addition of PMA) for another 48 h. It was discovered that macrophages polarized into M1, M2a, or M2c after being exposed to 20 ng/mL LPS + IFN-γ for 24 h, 25 ng/mL IL-4 + IL-13 for 72 h, and 1 μM hydrocortisone for 72 h. To remove carry-over cytokines, LPS, and hydrocortisone, polarised macrophages were thoroughly washed and incubated in fresh media for 24 h. The expression of markers CD206, CD163, CD23, and CD80 (BioLegend, San Diego, CA, USA) were used to decide the macrophage subspecies using a BD Accuri C6 flow cytometry. The mRNA expression levels of some genes (CXCL-1, CXCL-3, CCL-22, CCL-24, IL-1β, IL-8, IL-18,

TGF-β) were determined using a real-time polymerase chain reaction (RT-PCR) method to show the polarisation of M0, M1, M2a, and M2c subtypes. Finally, macrophages M0, M1, M2a and M2c were photographed with the Leica DM inverted light microscope to assess morphology.

WST-1 cytotoxicity test

WST-1 assay (Roche) was used to determine cell viability. M0 macrophages were cultured at a density of 1×10^4 cells per well into 96-well plates. Cells were treated with bortezomib and ixazomib at different concentrations for 24 and 48 h. After incubation, wells were filled with WST-1 cell proliferation reagent (10 µl/well) and absorbances (420 nm) were measured after 3 h. The absorbance of the samples was measured using a Cytation 3 Multi-mode reader (BioTek, Winooski, VT, USA). The absorbance was related to the number of living cells, and cell viability was represented as a percentage of controls [20, 23].

Proliferation assay by real-time cell analysis system

The real-time cell analysis system (RTCA DP) system continuously monitors cell behavior by measuring the impedance changes of attached cells and providing a cell index (CI) value. During the experiment days, the impedance of the wells for each group and concentration was measured every hour and defined as a CI value. We searched at cell proliferation as well as the IC_{50} concentrations of bortezomib and ixazomib. The cells were then seeded at a density of 1×10^4 per well in 16-well E-plates in 100 µl medium. After 24 h of incubation, the xCELLigence RTCA DP Instrument measured the impedance of each well every hour (ACEA Biosciences, USA). In the final step, the instrument was stopped, and medium was removed from the wells containing bortezomib and ixazomib at several concentrations. Assays were run in 8 wells, and the average values were calculated. Cell proliferation and IC_{50} concentrations of bortezomib and ixazomib were monitored and evaluated for 48 h according to the CI values by RTCA DP Software 1.2.1 [24, 25].

Co-culture procedures

THP-1 polarised M1, M2a or M2c were co-cultured with A549 lung cancer cells in indirect contact via transwell inserts (Corning, NY, USA) to investigate the impact of M1, M2a, and M2c on cancer cell sensitivity to proteasome inhibitors. The A549 cells were co-cultured with M1, M2a, and M2c macrophages in six-well plate cell culture inserts with a 0.4 µm porous membrane separating the upper and lower chambers, allowing for the exchange of soluble factors but not cell transmigration. To ensure consistency between experiments, THP-1 cells were plated in the upper chamber at a 5:1 ratio to the number of A549 cells plated in the lower chamber. The THP-1 cells were seeded into the transwell apparatus's upper chamber, stimulated to differentiate into M0 macrophages by adding 100 ng/mL PMA for 24 h washed with PBS, and incubated for another 48 h to eliminate the effect of PMA. The attached cells, which corresponded to M0 macrophages, were polarised into M1, M2a, or M2c macrophages by adding 20 ng/mL LPS + IFN-γ for 24 h, 25 ng/mL IL-4 + IL-13 for 72 h, and 1 µM hydrocortisone for 72 h. A549 cells were seeded in the lower chamber 24 h before macrophage polarisation ended. The upper chambers containing the M1, M2a, or M2c macrophages were then placed directly on top of the A549 cells in the six-well plates. The two cell populations were incubated for 48 h with bortezomib and ixazomib IC_{50} concentrations added directly into the wells.

Real-time monitoring of A549 cell proliferation under co-culture conditions with M1, M2a or M2c polarised macrophages using the E-plate insert

The E-Plate insert allows for real-time analysis of specific cell–cell interactions while keeping the cells separated in compartments. A 0.4 µm pore size membrane separates two different cell populations, allowing control of physical contact and interaction duration. Briefly, A549 cells were seeded in E-plate at a density of 1×10^4/well with culture medium and incubated in the RTCA cradle for 24 h. Until the end of the experiment, hourly impedance signals were recorded. After 24 h of incubation, the E-plates were taken to the RTCA unit where 160 µL of culture medium was replaced with 80 µL of SFM for the control (For the bortezomib and ixazomib groups, IC_{50} concentrations are determined in SFM). The inserts were gently lowered into the E-16 plate (the insert consists of 80 µL SFM with M1, M2a, or M2c polarised macrophages). The control group consisted of a well with no cells seeded in the same insert(s). The impedance recording was then resumed on the device for the duration of 48 h. Four wells were used for each treatment group.

Apoptosis detection using Annexin V-FITC and propidium iodide staining

A549 cells (2×10^5/well) were placed in 6-well plates before being co-cultured with macrophages in SFM at a cell density of 1:5. A549 cells and M1, M2a or M2c co-culture groups were incubated with bortezomib and ixazomib IC_{50} concentrations for 48 h. A549 cell analysis was conducted according to the Annexin V-FITC Apoptosis Detection Kit procedure, used to detect apoptosis as described previously [20]. Finally, the samples were diluted with 250 µL of the

binding buffer, processed for data acquisition, and analysed on a BD Accuri™ C6 Flow Cytometry; at least 1×10^4 cells were analysed per sample.

Detection of caspase-3 activity

Caspase-3 is an essential protease that initiates apoptosis [20, 26]. Alterations of the caspase-3 level of cells were determined using the PE Active Caspase-3 Apoptosis Kit procedure, used to detect caspase-3 levels as described previously [20]. A549 cells and M1, M2a or M2c co-culture groups were incubated with bortezomib and ixazomib IC_{50} concentrations for 48 h. After incubation, the samples were analyzed using BD Accuri™ C6 Flow Cytometry. At least 1×10^4 cells were analysed per sample.

Determination of loss of mitochondrial membrane potential by JC-1 dye using flow cytometry

A549 cells and M1, M2a or M2c co-culture groups were incubated with bortezomib and ixazomib IC_{50} concentrations for 48 h. We used the Flow Cytometry JC-1 dye Kit to evaluate at the decrease of mitochondrial membrane potential in response to ixazomib and bortezomib in cells, as described before [20, 26]. After incubation, the samples were analyzed using BD Accuri™ C6 Flow Cytometry. At least 1×10^4 cells were analysed per sample.

Cytokine detection

A549 cells (2×10^5) were seeded in 6-well plates 24 h before the end of polarisation. A549 cells and M1, M2a or M2c co-culture groups were incubated with bortezomib and ixazomib IC_{50} concentrations for 48 h. At the end of the incubation, supernatants were collected from the co-culture. The BD human inflammatory kit procedure was used to measure TNF-α and IL-10 cytokine levels (BD™ Cytometric Bead Array [CBA] Human Inflammatory Cytokines Kit, Catalogue Number: 551811). A FCAP array was used in a BD Accuri C6 flow cytometer for CBA analysis.

Quantitative RT-PCR

Total RNA was extracted from M1, M2a, or M2c macrophages to determine the expression of M1 and M2 macrophage markers, from A549 lung cancer cells to assess single-cell control, and from co-cultured A549 cells and macrophages to determine the change in genes in the EMT pathway. RNA was extracted using a MagNA Pure Compact RNA Isolation Kit for the MagNA Pure Compact Instrument LC 2.0 system (Roche Diagnostics, Mannheim, Germany). Reverse transcription was performed using a High-Fidelity cDNA Synthesis Kit (Roche, Germany). A NanoDrop spectrophotometer was used to verify the RNA samples' purity. For cDNA synthesis, 500 ng of RNA were taken from each RNA population. Real-time PCR was performed using the SYBR Green Master Mix (Roche Applied Science, Germany) on a LightCycler® 480 instrument (Roche Applied Science, Germany). The internal control was glyceraldehyde 3-phosphate dehydrogenase (GAPDH). Table 1 shows the primer sequences that were used. The results were normalized to GAPDH expression levels and presented as averages of three experiments.

Immunofluorescence staining of vimentin and E-cadherin

Vimentin and E-cadherin levels in the A549 control and M2a and M2c co-culture groups were analysed by flow cytometry (Accuri C6, BD). The M2c macrophage co-culture groups found to be more significant, vimentin and E-cadherin levels were investigated by immunofluorescence staining in the Cytation 3 Cell Imaging Multimode Reader. An Immunofluorescence Application Solutions Kit (Cell Signaling) was used for the fixation, permeabilisation and immunostaining of antibodies to determine the levels of E-cadherin and vimentin in the cells. The vimentin antibodies (vimentin [D21H3] XP® rabbit mAb, Cell Signaling) were diluted 1:100 and E-cadherin monoclonal antibodies (E-cadherin [4A2] mouse mAb, Cell Signaling) were diluted 1:50. Overnight at 4 °C, the cells were incubated with 100 µl of antibody. After incubation, secondary antibody Anti-rabbit Alexa Fluor 594 (anti-rabbit IgG [H + L], F(ab')2 Fragment, Cell Signaling) at a 1:500 dilution. Secondary antibodies (anti-mouse Alexa Fluor 488, ab150113, Abcam) were added to the wells and incubated for 1 h at room temperature. Hoechst 33,258 (10 µg/mL) was used to stain the cell nuclei 10 min before imaging with Cytation 3 Cell Imaging Multi-Mode Reader [27].

3D culture studies

Culturing cells with AlgiMatrix

Cells (2×10^4/well) were incorporated into alginate scaffold in 100 µL of media to determine the optimal time for spheroids formation. After 20 min, a further 100 µL of media was added, and the cells were grown in an incubator at 37 °C with 5% CO_2 for another 20 min. Every 48 h, the media was changed. To assess growth, tumor spheroids were observed in alginate scaffold wells 3, 5, and 7 days after cell seeding. Images were taken using an inverted microscope (Leica DM 300), and the size of spheroids was determined by the Leica LAS Analysis program. Also, cell spheroids were imaged by Hoechst fluorescent dye.

Table 1 Real-Time nucleotide primer sequence

Genes	Short name	Forward Primer- Reverse Primer
Interleukin-1 Beta	IL-1β	Forward: 5'-AAGATGCTGGTTCCCTGCC-3' Reverse: 5'-GCGTGCAGTTCAGTGATCGTAC-3'
Interleukin -8	IL-8	Forward: 5'-CCGGAAGGAACCATCTCACT-3' Reverse: 5'-ACTTCTCCACAACCCTCTGC-3'
Interleukin -18	IL-18	Forward: 5'- GATAGCCAGCCTAGAGGTATGG -3' Reverse: 5'- CCTTGATGTTATCAGGAGGATTCA -3'
Chemokine Ligand-1	CXCL-1	Forward: 5'- AGCTTGCCTCAATCCTGCATCC -3' Reverse: 5'- TCCTTCAGGAACAGCCACCAGT -3'
Chemokine Ligand-3	CXCL-3	Forward: 5'- TTCACCTCAAGAACATCCAAAGTG-3' Reverse: 5'- TTCTTCCCATTCTTGAGTGTGGC -3'
Transforming Growth Factor Beta	TGF-Beta	Forward: 5'- TACCTGAACCCGTGTTGCTCTC-3' Reverse: 5'- GTTGCTGAGGTATCGCCAGGAA-3'
Chemokine Ligand-22	CCL-22	Forward: 5'- TCCTGGGTTCAAGCGATTCTCC -3' Reverse: 5'- GTCAGGAGTTCAAGACCAGCCT -3'
Chemokine Ligand-24	CCL-24	Forward: 5'- TGAGAACCGAGTGGTCAGCTAC -3' Reverse: 5'- TTCTGCTTGGCGTCCAGGTTCT -3'
Glyceraldehyde-3 phosphate dehydrogenase	GAPDH	Forward: 5'- GTCAAGGCTGAGAACGGGAA -3' Reverse: 5'- AAATGAGCCCCAGCCTTCTC -3'
Vimentin	VIM	Forward: 5'- GGACCAGCTAACCAACGACA -3' Reverse: 5'- AAGGTCAAGACGTGCCAGAG -3'
Fibronectin	FN1	Forward: 5'- CCCTGATTGGAACCCAGTCC -3' Reverse: 5'- CTGTCACACGAGCCCTTCTT -3'
E-Cadherin	CDH1	Forward: 5'- AGCTCTGCTGCCTCGTCTAT -3' Reverse: 5'- GGCCTCTCTTGGTTAGGAGG -3'
Nuclear Factor Kappa B	NF-kB	Forward: 5'- CGCCGCTTAGGAGGGAGA -3' Reverse: 5'- GGTATGGGCCATCTGCTGTT -3'
Vascular Endothelial Growth Factor	VEGF-A	Forward: 5'- GCAAGACAAGAAAAATGTGACAA-3' Reverse: 5'- TGGTTTCTGTATCGATCGTTCT-3'
Chemokine ligand -17	CCL-17	Forward: 5'- TGTTCGGACCCCAACAACAA -3' Reverse: 5'- TAGTCCCGGGAGACAGTCAG -3'

Transcripts Primer forward Primer reverse

Comparison of 2D and 3D cytotoxicity data of bortezomib and ixazomib

Based on the preliminary experiments, the more abundant spheroid formation was observed in the 7-day culture. As a result, 7 days was chosen as the starting point for treatment. The treatment included the use of bortezomib and ixazomib at various concentrations (0.1–400 μM). After 48 h incubation, for WST-1 viability determination, sponges were dissolved using an AlgiMatrix Dissolving Buffer, which provides a quick and straightforward way to recover cells from the AlgiMatrix bioscaffold. After 3 h, wells were filled with the cell proliferation reagent WST-1, and absorbances were measured. 2D culture studies were also conducted in parallel with this experiment. IC_{50} values were then calculated for both 2D and 3D cultures using MS Excel.

Statistical analysis

The results were analyzed using one-way ANOVA and Tukey's post hoc test in Graphpad Prism 6.0. The means of three independent experiments are expressed as mean standard deviation (±). The significance of the results in comparison to the control group is represented by P values ($P > 0.05$ n.s, $P < 0.05$*, $P < 0.01$**, $P < 0.001$***, and $P < 0.0001$****).

Results

Monocytic THP-1 cells differentiation into M0 macrophages

THP-1 cells grew in suspension as single cells or partially in clusters and had a wide and round morphology (Fig. 1a). THP-1 cells were differentiated into macrophages after 24 h of stimulation with 100 ng/mL PMA. During differentiation,

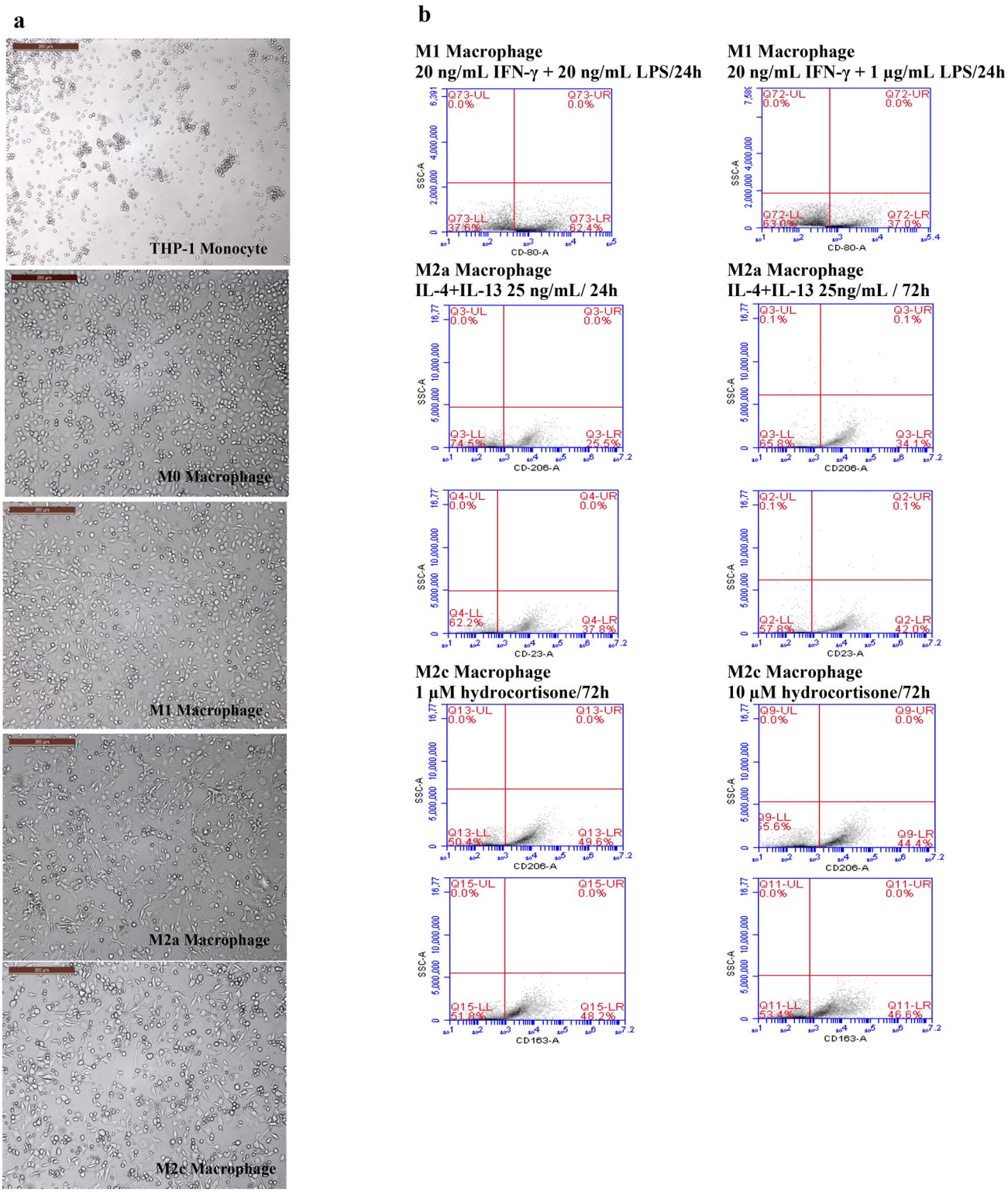

Fig. 1 M1, M2a and M2c macrophage polarization (**a**) Light microscope image of THP-1, THP-1 origin macrophage (M0), M1, M2a and M2c polarized macrophage cells (10X). **b** Validation of M1, M2a/c polarization by the flow cytometry. CD80, CD23 and CD163 are specific surface markers of M1, M2a and M2c macrophages, respectively, and the marker CD206 is common to both M2 subtypes. Experiments were performed in triplicate. **c** Expressions of some M1/M2 markers in differentiated macrophage subtypes, determined by RT-PCR. The gene expression of differentiated macrophage subtypes was normalized to that of untreated M0 macrophages. $p < 0.05$*, $p < 0.01$**, $p < 0.0001$****, (mean ± SD, n = 3)

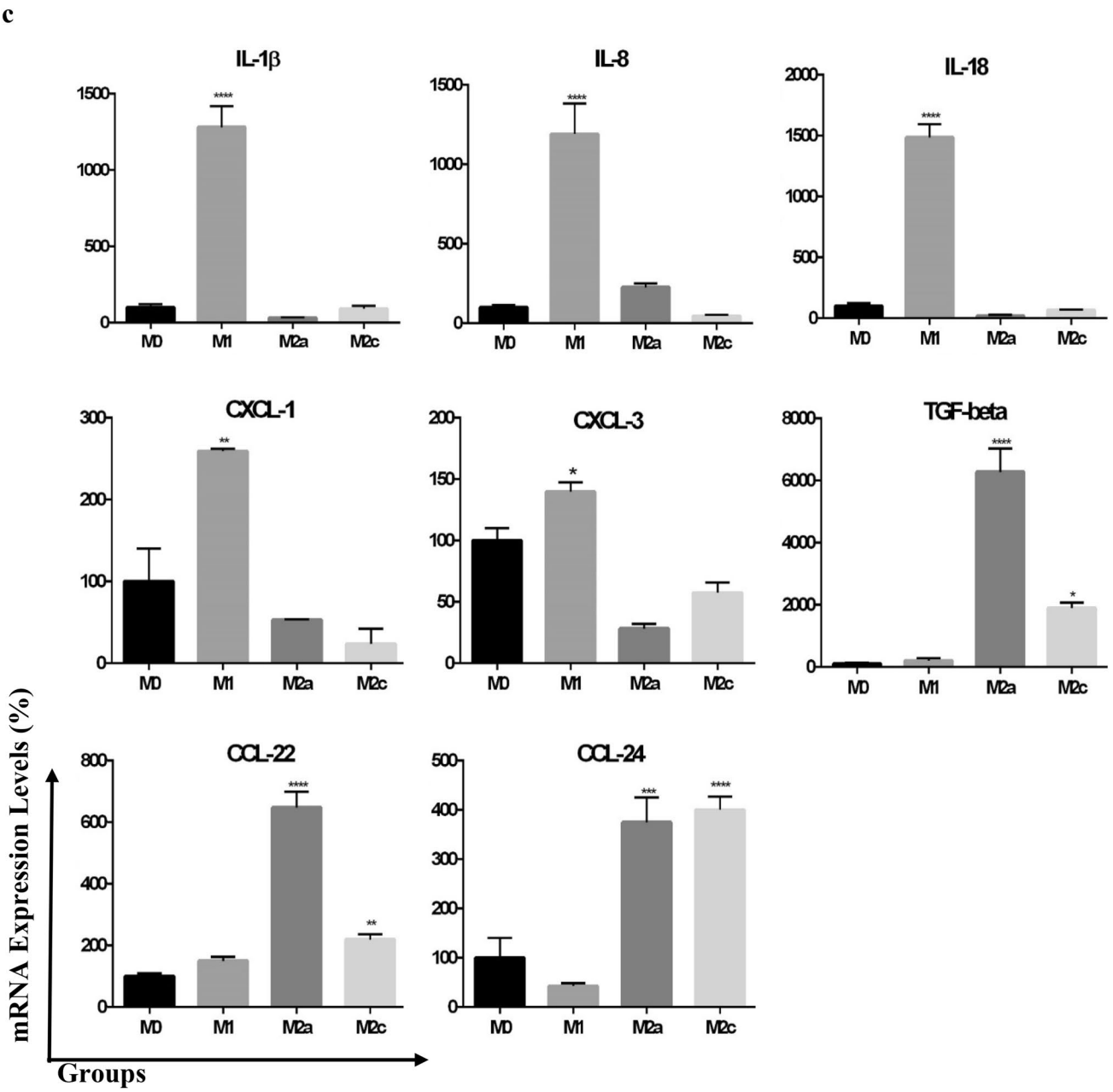

Fig. 1 (continued)

the cells attached to the flask bottom changed shape from round to almost spindle-shaped, and pseudopods appeared in some cells. Due to the fact that all macrophage populations express CD68, different PMA concentrations and incubation times were used to determine differentiation. Based on our flow cytometry results, we chose a 24-h incubation with 100 ng/mL PMA, followed by a 48-h rest period (CD-14 [5.5%] and the CD-68 [58.2%] levels were determined, data not shown).

THP-1 polarisation into pro-inflammatory M1 macrophages

According to numerous studies, macrophages polarize to the M1 phenotype in the presence of IFN-γ and in combination with inflammatory stimuli such as LPS [9, 28]. Based on these data, we tested various concentrations of LPS (20 ng/mL or 1 μg/mL), combined with 20 ng/ml of IFN-γ, and incubated THP-1 macrophages for 24 h. Macrophage M1 polarisation was assessed by measuring the mRNA expression of M1 markers, pro-inflammatory cytokines IL-1β,

IL-8, IL-18, CXCL1 and CXCL3, using RT-qPCR and CD80 membrane receptors level by flow cytometry. Based on our CD80 results, we chose 20 ng/mL IFN-γ and 20 ng/mL LPS for M1 polarization during the 24-h incubation period. An increased pro-inflammatory marker (IL-1β, IL-8, IL-18, CXCL1 and CXCL3) expression profile was obtained by incubation with IFN-γ combined with 20 ng/mL LPS in comparison to M0 macrophage (Fig. 1b). Additionally, we examined the mRNA expression of some M2 markers (TGF-Beta, CCL22, and CCL24) in M1 macrophages and found that these genes were not significantly expressed. Finally, incubating THP-1 macrophages (M0) for 24 h with IFN-γ 20 ng/mL and LPS 20 ng/mL causes them to polarize into M1 macrophages.

THP-1 polarisation into anti-inflammatory M2a and M2c macrophages

We incubated M0 macrophages with IL-4 and IL-13 at a concentration of 25 ng/mL or hydrocortisone at 1 and 10 μM for 24 or 72 h. The M2a and M2c macrophages were characterised by CD206 (M2 marker), CD23 (M2a marker) and CD206, CD163 (M2c marker) membrane receptor levels by flow cytometry, respectively (Fig. 1b). Incubation of THP-1 macrophages (M0) with IL-4 and IL-13 (25 ng/mL) and hydrocortisone (1 μM) for 72 h induces their polarisation into M2a and M2c macrophages, respectively. Furthermore, mRNA expression levels of some M2 markers (TGF-β, CCL-22 and CCL-24) were increased in M2a and M2c macrophages compared to M0 macrophage (Fig. 1c).

Antiproliferative effects of bortezomib and ixazomib determined by RTCA DP

RTCA DP detects the cell number indirectly by measuring electrical impedance and generates real-time data by collecting measurements at predetermined intervals over a period of days [23]. In our study, the RTCA DP system was used for the real-time and time-dependent analysis of IC_{50} concentrations of A549 and CCD-19Lu cells. The WST-1 method was used to select the appropriate concentrations of bortezomib and ixazomib for evaluation in the xCELLigence system (data not shown). Figure 2 shows that bortezomib and ixazomib decreased the viability of A549 and CCD-19Lu cells in a dose-dependent manner. Also, to compare the cytotoxic effects of the bortezomib and ixazomib on A549 lung cancer and CCD-19Lu healthy lung fibroblast cells, their IC_{50} values were calculated after 48 h exposure. The IC_{50} value determined for bortezomib and ixazomib in A549 lung cancer cells was found to be lower than the IC_{50} value determined for CCD-19Lu cells. IC_{50} concentrations of bortezomib and ixazomib (45 nM and 2 μM, respectively) were determined and applied to macrophages during the co-culture process, and macrophage viability was determined by the WST-1 method. Bortezomib and ixazomib had no significant cytotoxic effect on M0 macrophages at 24 and 48 h incubation (Fig. 2c).

M1 macrophages reduced A549 cell viability and proliferation while increasing drug sensitivity to bortezomib and ixazomib.

Numerous studies demonstrate that interactions with tumor-associated macrophages can influence cancer cell proliferation and chemosensitivity [28]. There is no other study using macrophage polarization co-culture and a real-time cell analysis system in the literature. The E-plate insert allows for real-time cell–cell interactions while keeping cells apart. Proliferation results were determined more precisely because A549 cells were located in the same culture medium as the E-plate insert used in co-cultures with M1, M2a or M2c polarised macrophages and their proliferation was measured in real-time (Fig. 3). A549 and M1 macrophage co-culture groups significantly decreased A549 cell viability and proliferation relative to the A549 control (Fig. 3a). Also, the results showed that the antiproliferative effects of bortezomib and ixazomib were higher in the A549 and M1 macrophage co-culture groups (Fig. 3b). We used annexin V/PI method, caspase-3 levels, and JC-1 assays to determine whether the reduced cell number of A549 cells exposed to M1 was due to apoptosis. M1 co-culturing for 48 h induced apoptosis in A549 cells, according to annexin V/PI staining. When A549 cells were incubated with M1 macrophages in the lack of drugs, there was an increase in apoptosis. Notably, bortezomib and ixazomib induced apoptosis most frequently in the M1 macrophage co-culture group. When A549 cells were incubated with M1 macrophages, the level of caspase-3 was higher than when the cells were incubated alone. In comparison to the control group incubated with bortezomib and ixazomib without macrophages, M1 macrophages significantly increased caspase-3 activity. M1 macrophages also increased caspase-3 activity in A549 cells treated with bortezomib and ixazomib. The observed loss of mitochondrial depolarisation also supports these findings. When A549 cells were incubated with M2a or M2c macrophages, the apoptosis of cancer cells did not change compared to the control group. Furthermore, JC-1 depolarisation was much less common in cells incubated with M2, particularly M2a. However, M2a and M2c macrophages increased the A549 cell apoptosis induced by bortezomib and ixazomib for all three apoptosis-related experiment results (Fig. 3c). Overall, these findings indicate that macrophages M1, M2a, and M2c modulated the apoptotic response to the proteasome inhibitors bortezomib and ixazomib in A549 cells.

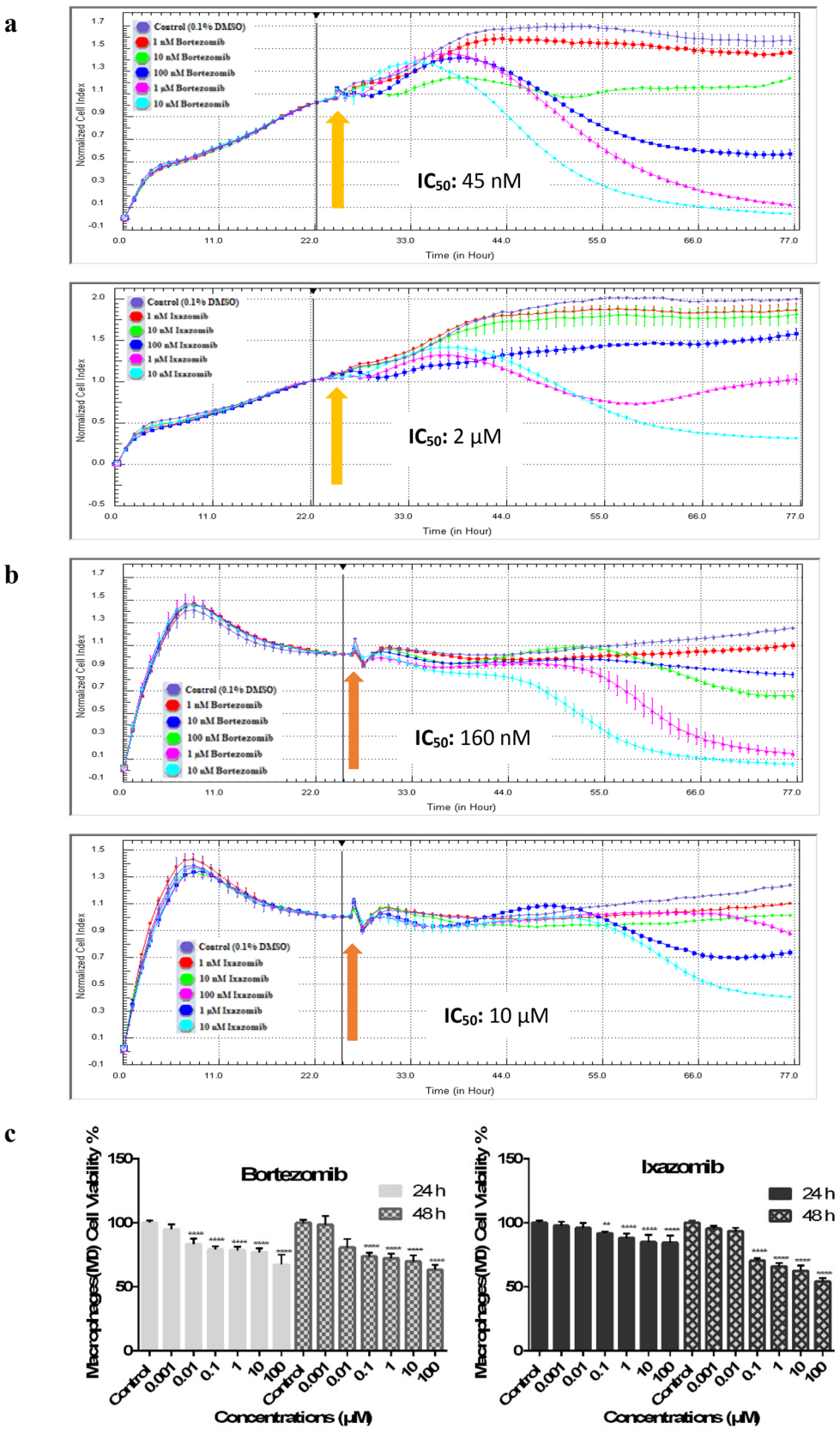

Fig. 2 Anti-proliferative effects of bortezomib and ixazomib on cells **a** A549 cell proliferation curves at 48 h of bortezomib (IC_{50}: 45 nM) and ixazomib (IC_{50}: 2 µM) concentrations, and A549 cell proliferation curves at 48 h of ixazomib concentrations, IC_{50}: 2 µM. **b** CCD-19 Lu cell proliferation curves at 48 h of bortezomib (IC_{50}: 160 nM) and ixazomib (IC_{50}: 10 µM) concentrations (Arrow: application of concentration point, mean ± SD, n = 6). **c** Concentrations of bortezomib and ixazomib in M0 macrophage cells and statistical assessment of the 24 and 48 h percent viability values calculated using the WST-1 method. $p < 0.01$**, $p < 0.0001$****, (mean ± SD, n = 8)

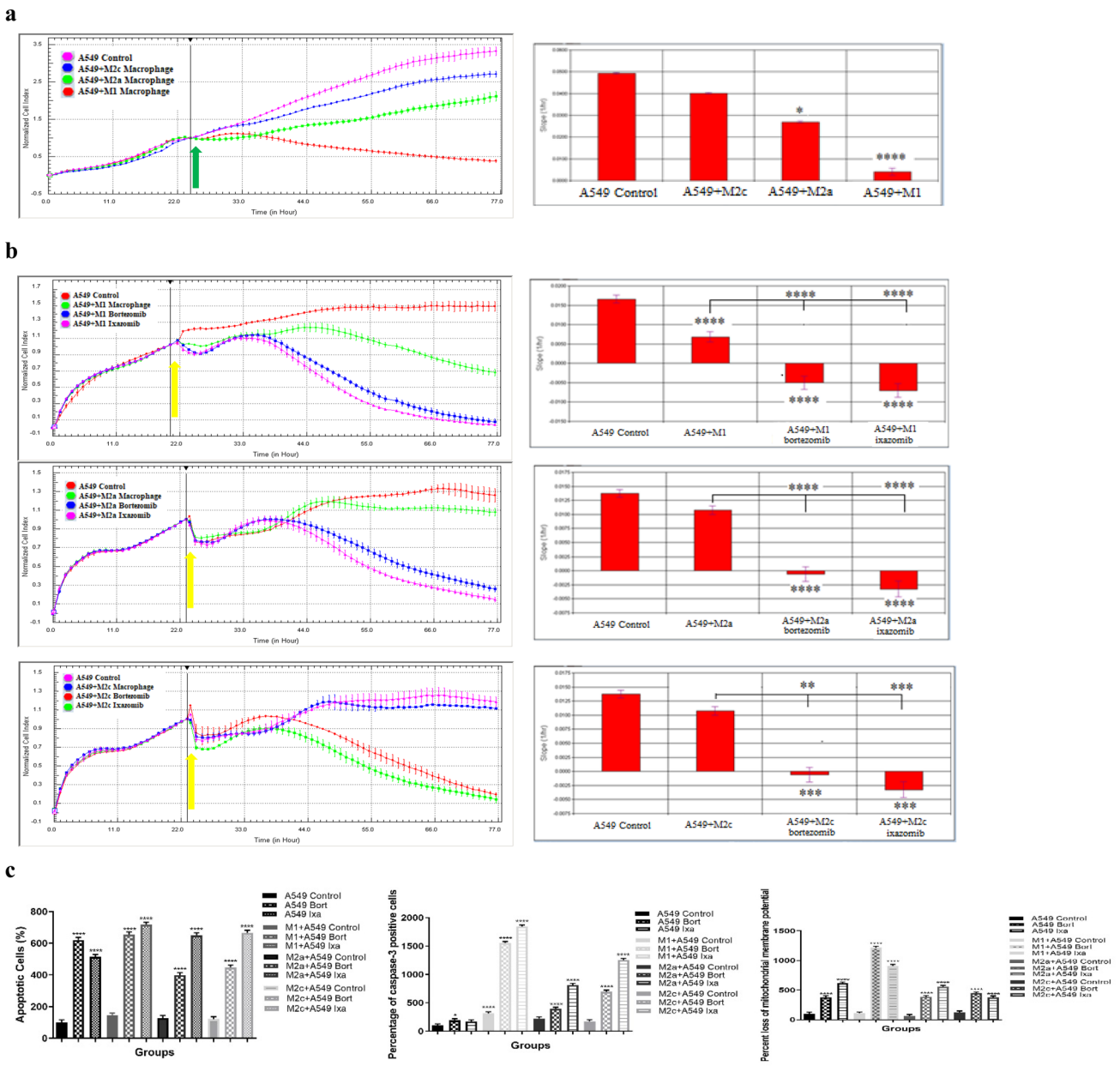

Fig. 3 Antiproliferative and apoptotic effects of macrophages on A549 cells **a** Proliferation curves and slope graph of co-culture models created with A549 and M1, M2a and M2c polarized macrophage cells using an E-plate insert, determined in a real-time cell analysis system (Arrow: merge of A549 and macrophages, mean ± SD, n = 6, $p < 0.05$*, $p < 0.0001$****). **b** Proliferation curves and slope graph of bortezomib and ixazomib IC_{50} concentrations at 48 h in the A549 and M1, M2a or M2c polarized macrophage co-culture model (Arrow: merge of A549 and macrophages and application of concentration point, mean ± SD, n = 6, $p < 0.01$**, $p < 0.001$***, $p < 0.0001$****). **c** Apoptosis of A549 cells and co-culture macrophage with bortezomib and ixazomib IC_{50} concentrations at 48 h or without drugs. Cell apoptosis was determined by flow cytometry with annexin V/PI-staining. Data were confirmed in three independent experiments (mean ± standard deviation, $p > 0.05$, $p < 0.0001$ ****). Caspase-3 activity A549 cells and co-culture macrophage with bortezomib and ixazomib IC_{50} concentrations at 48 h or without drugs determined by flow cytometry. Data were confirmed in three independent experiments and the error bars show the standard deviation ($p > 0.05$, $p < 0.05$*, $p < 0.001$***, $p < 0.0001$****). Mitochondrial membrane depolarization of A549 cells was determined at 48 h by flow cytometry with JC-1 staining. Data were confirmed in three independent experiments and the error bars show the standard deviation ($p < 0.0001$****)

M2c macrophages induced the EMT of lung A549 cancer cells

To determine whether the EMT pathway was activated, TNF-α and IL-10 cytokine levels were determined from A549 cell supernatants and M1, M2a and M2c polarised

macrophage co-culture groups using flow cytometry. IL-10 cytokines increased in co-culture groups formed by both M2a and M2c polarised macrophages and A549 cells, and there was a significant increase in the M2c macrophage co-culture group ($p < 0.01$**) (Fig. 4a). mRNA expression levels of EMT-related factors (vimentin, fibronectin, E-cadherin, NF-kB, VEGF, and CCL-17) in A549 cells were evaluated in a co-culture model of M1, M2a and M2c polarised macrophages. The most important mesenchymal factors, vimentin, and fibronectin increased, and E-cadherin decreased in both A549 M2a and M2c macrophage co-culture groups. Also, no significant changes in vimentin, fibronectin, E-cadherin, NF-kB, VEGF, and CCL-17 mRNA expression were found in the M1 macrophage groups. mRNA expression levels of CCL-17 did not change significantly in the M1 polarised macrophage co-culture group, but they decreased in the M2a macrophage group compared to the A549 control group ($p < 0.05$*). A significant increase ($p < 0.0001$****) in the M2c macrophage co-culture group was distinct as it indicated that EMT increased the most in the M2c polarised macrophage co-culture group (Fig. 4b). Based on these findings, it was determined that EMT was induced in M2c macrophage A549 co-culture groups. This result is supported by the increased vimentin and decreased E-cadherin levels determined by flow cytometry (Fig. 4c). Proteasome inhibitors have also been found to reduce EMT by decreasing vimentin, NFkB, VEGF, and CCL-17 expression levels. Especially for ixazomib, the reduction of EMT was statistically more significant than bortezomib. In addition, vimentin, and E-cadherin in M2c co-culture groups, as imaged by immunofluorescence staining images (Fig. 4d), show an increase in vimentin (red) and a decrease in E-cadherin (green) monoclonal antibody levels in the A549 and M2c co-culture group compared to the A549 control group. Finally, it was determined that bortezomib and, more so, ixazomib decreased M2c-induced EMT in A549 lung cancer cells.

Optimisation of 3D A549 Lung Cancer Spheroids

3D culture environment was created using the AlgiMatrix® 3D Culture System. Based on the type of cells incorporated, the spongy features of the AlgiMatrix® system provide the needed place for cells to grow as models of in vitro solid tumors include lung cancer [29]. Figure 5 shows spheroid areas and morphological images of randomly selected A549 cells on days 3, 5, and 7. The graph generated by the average spheroid area (μm^2) was obtained from A549 cell images taken on different days (Fig. 5b). The spheroid area increased statistically on day 7 ($p < 0.0001$****).

Comparative analysis of IC_{50} values of bortezomib and ixazomib in 2D and 3D systems

3D cultures are known for accurately replicating the physiologic microenvironment and having a high level of harmony with in vivo conditions. In our study, we aimed to determine IC_{50} concentrations for proteasome inhibitors to shed light on in vivo models by taking advantage of 3D culture. The IC_{50} values for bortezomib and ixazomib were significantly higher in AlgiMatrix systems than in 2D culture models. After 48 h of A549 incubation with bortezomib and ixazomib, the IC_{50} value in 3D culture was approximately 15 times higher for bortezomib and 9 times higher for ixazomib than in 2D culture (Table 2).

Discussion

Lung cancers are initiated and metastasize not only due to their genetic and molecular characteristics but also due to their interaction with the immune system and the tumor microenvironment [30]. In solid tumours, TAMs comprise 5–40 percent of the total tumor mass in most cases. Furthermore, there is usually a link between the number of TAMs and the specific condition, depending on the type of tumor [5]. In response to a stimulus in their environment, macrophages can be differentiated into M1 or M2 macrophages. Recent research suggests that macrophage polarization may be used as a therapeutic strategy in the treatment of cancer and angiogenesis [13, 28]. Previous studies have mostly focused on M1 macrophages, and no subtype distinction has been observed in M2 macrophages.

There are limited data available on M2c macrophages. In this study, we found that macrophages with M1, M2a, and especially M2c polarization had different effects on lung cancer cell apoptosis, the EMT pathway, and gene expression profiles. In several studies, M2a polarisation has been reported to occur in the presence of IL-13 and IL-4 [31–33]. Concentrations of IL-14 and IL-13 used in these studies were in the range of 20–25 ng/mL, and incubation times were 24, 48 and 72 h [34, 35]. In the limited amount of previously published data, especially on M2c polarised macrophages, IL-10 (20 ng /mL) has been used during the differentiation of THP-1 cells into M2c macrophages [28, 36]. No previous study has utilised hydrocortisone to polarise M2c cells. Notably, we used hydrocortisone for the first time in M2c polarisation by focusing more on M2 macrophages. M2 macrophages are polarised to M2c macrophages by different stimuli. Although M2c macrophages are reported to be polarised with IL-10, TGF- and glucocorticoids [8, 37], no studies to date have reported polarisation using the glucocorticoid hydrocortisone. We optimised hydrocortisone polarisation of M2c for the first time in this study, identifying

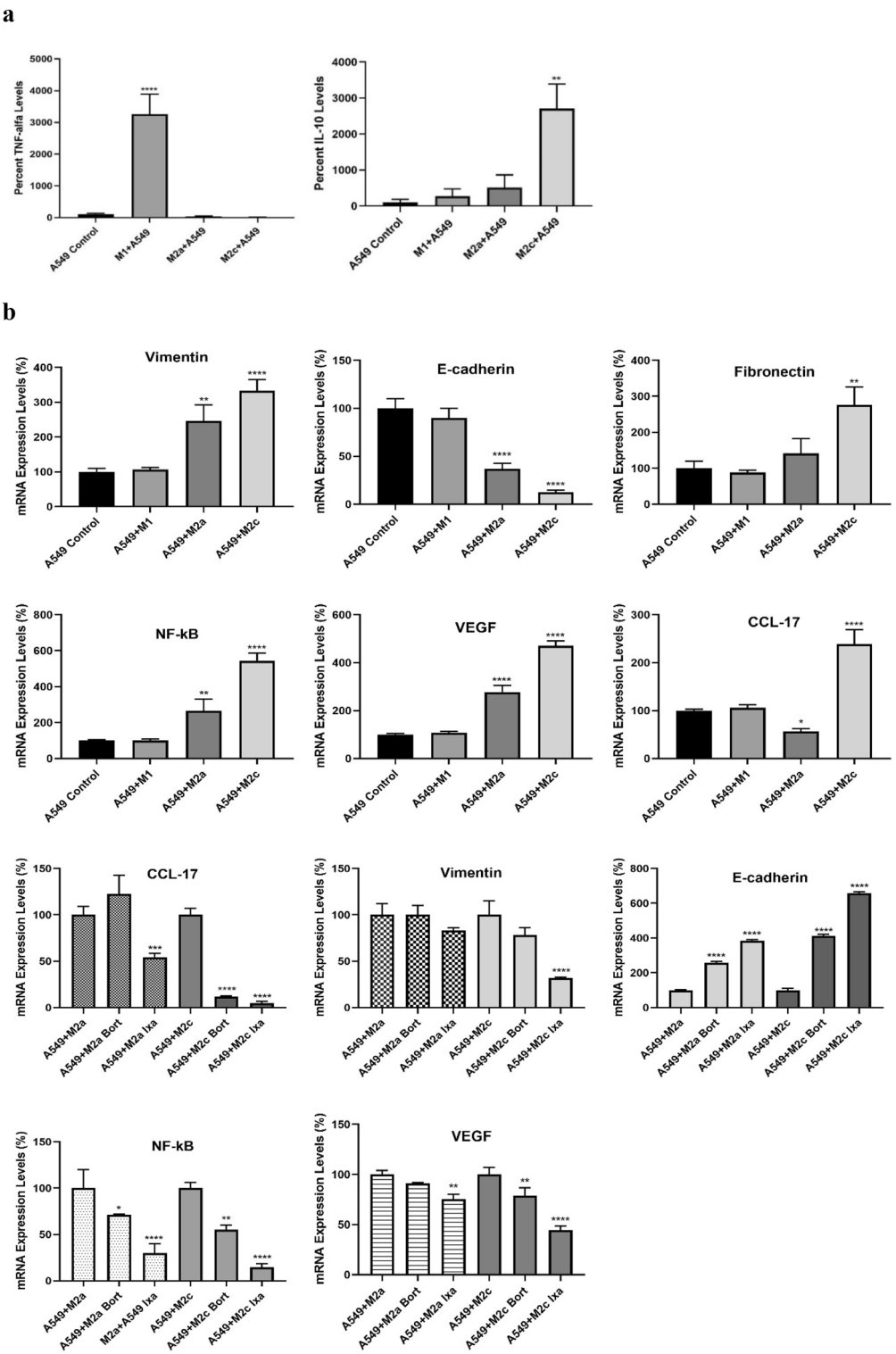

Fig. 4 M2c macrophages induced EMT **a** TNF-α and IL-10 cytokine levels (percentage) evaluated by flow cytometry in A549 cells and M1, M2a and M2c polarized macrophage co-culture groups (n = 3, mean ± SD, p < 0.01**, p < 0.0001****). **b** Expressions of some EMT markers in A549 cells co-cultured with M1, M2a and M2c polarized macrophage with or without drugs, determined by RT-PCR. p < 0.05*, p < 0.01**, p < 0.0001****, (mean ± SD, n = 3). **c** Vimentin and E-cadherin levels of A549 cells were determined by flow cytometry. In addition, the results of percent change and the statistical evaluation of vimentin and E-cadherin levels are shown in the graphic. Data were confirmed in three independent experiments and the error bars show the standard deviation (p < 0.05*, p < 0.01**, p < 0.0001****). **d** Morphological image of vimentin (red, Alexa Fluor 594) and E-cadherin (green, Alexa Fluor 488) in A549 cells undergoing immunofluorescence staining. Cell nuclei stained blue (with Hoechst 33,258). The data expressed as the mean values ± SD (p ≤ 0.001). Images were taken by Cytation 3 Cell Imaging Multi-Mode Reader with 10 × objective

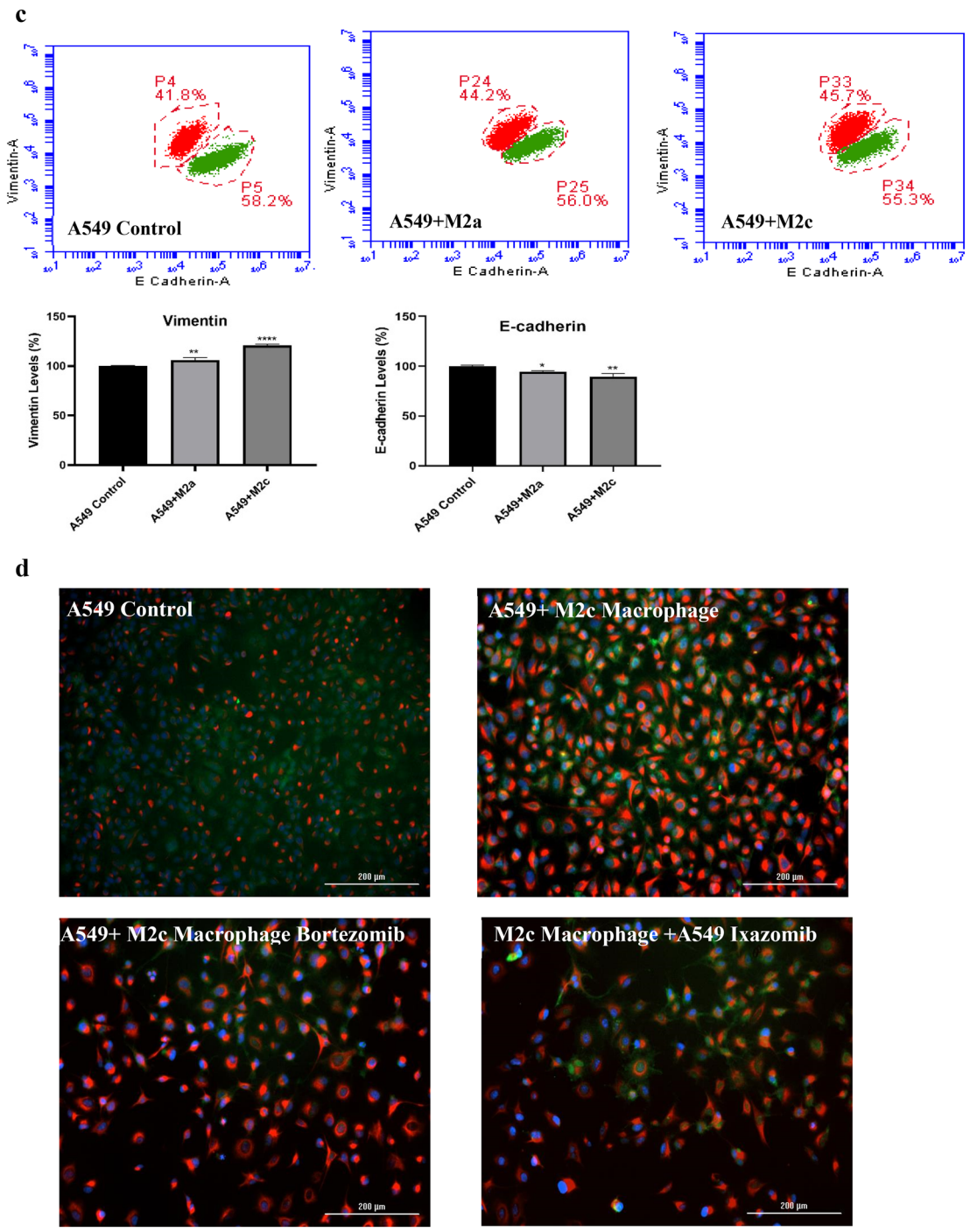

Fig. 4 (continued)

many surface markers (CD206 and CD163) and cytokines and observing chemokine gene expression (IL-1 β, IL-8, IL-18, CXCL-1, CXCL-3, CCL-22, CCL-24, TGF-β).

Numerous studies demonstrate that interactions with tumor-associated macrophages can influence cancer cell proliferation and chemosensitivity [28]. There is no other study using macrophage polarization co-culture and a RT-CA system in the literature on A549 cells. M1 macrophages have been shown in studies to inhibit tumor growth and increase the sensitivity of chemotherapy agents [28, 35]. We found that M1 polarised macrophages alone decreased A549 cell viability using the real-time cell analysis system. In addition, M1 macrophages alone affected and increased the bortezomib and ixazomib-induced apoptosis. Proteasome

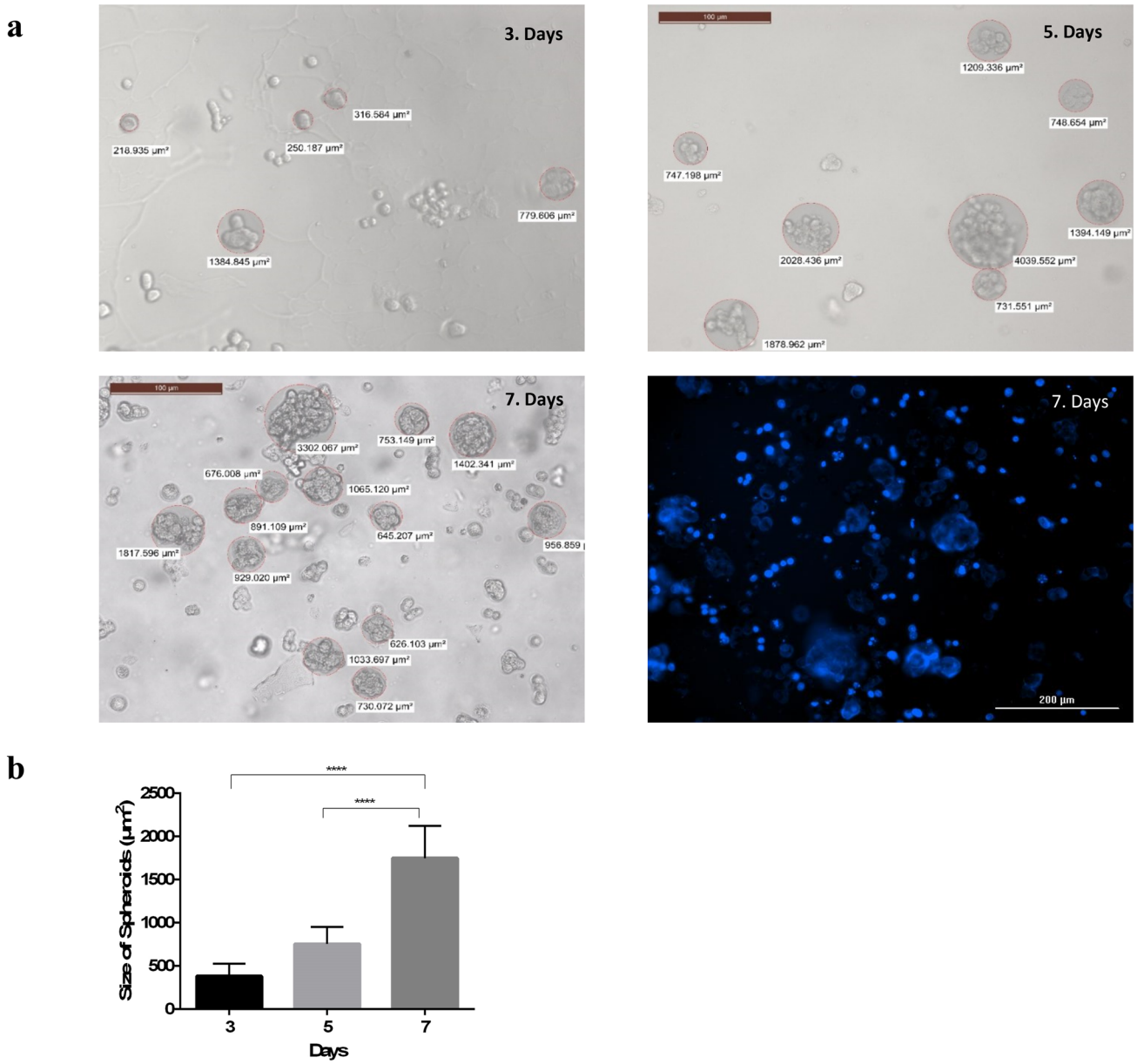

Fig. 5 3D culture studies **a** Morphological imaging of spheroids in A549 lung cancer cells. Also, spheroid formations of A549 cells were imaged as fluorescence in Cytation 3 Cell Imaging Multi-Mode Reader with Hoechst 33,258 on day 7 (10X). **b** Spheroid sizes obtained from cell images of A549 cells taken on different days (n = 25, mean ± standard deviation, $p < 0.0001$ ****) Random photos were taken for the analysis of the areas of the spheroids. A total of 25 photographs were selected among these photographs for each day, including 5 photographs with at least 5 spheroids

Table 2 IC_{50} values of bortezomib and ixazomib in A549 cells at 48 h in 2D and 3D cell culture

IC_{50} concentration (µM)	2D	3D
Bortezomib	6.32 µM	98.6 µM
Ixazomib	41,27 µM	353.01 µM

inhibitors have previously been reported to cause apoptosis in cancer cells [20, 21, 38, 39]. Although the apoptotic effect of ixazomib on lung cancer cells has not been previously investigated, its apoptotic effects have been observed on many other solid tumour cell lines (colon, prostate, hepatocellular carcinoma cells) [21, 40, 41].

EMT is a process in which cells morphologically transition from the epithelial phenotype to the mesenchymal fibroblastoid phenotype and plays an important role in the

cancer metastasis process [14]. TNF-α, released by M1 macrophages, is an important cytokine that modulates inflammatory responses in the microenvironment of many tumours [42]. Although studies have reported many factors, such as EGF, TGF-β, TNF-α, generally found in the tumour microenvironment, induce EMT [43], more recent studies have also reported that TNF-α inhibits EMT by suppressing TGF-β levels [44]. Furthermore, the TLR4/IL-10 axis has been implicated in the EMT signaling pathway, and inhibition of effectively suppresses EMT induction [45]. In our results, decreased TNF-α and increased IL-10 levels in A549 cells and M2a and M2c polarised macrophage co-culture are responsible for increased EMT in A549 cells. Also, EMT was induced in A549 cancer cells in co-culture groups formed with M2a and M2c macrophages, depending on the expression levels of vimentin, E-cadherin, fibronectin, NF-kB, VEGF and CCl-17 mRNA. An increase in TGF-β mRNA expression is a particularly relevant result because studies have shown that TGF-β is an important factor for EMT and can be an EMT-inducing agent [44, 46]. According to our results, TGF-β may play a role in the induction of EMT in A549 cells with co-culture of M2a and M2c macrophages.

Factors such as CCL-17 derived from tumour-associated macrophages are important contributors to immunosuppression. Studies have shown that this causes and intensifies various stages of cancer progression [47]. The high levels of CCL-17 mRNA expression levels found only in the M2c macrophage and A549 co-culture group are informative.

NF-kB is a key transcriptional factor responsible for regulating the inflammatory signal and is important in cellular proliferation and differentiation. It's a key marker for cancer invasion and EMT, and it's involved in both the induction and support of EMT. As a result, it has been proposed that NF-kB activity decreases the expression of genes associated with EMT [16, 17, 48]. We observed, bortezomib and ixazomib 'well-known NF-KB inhibitors' decreased M2c-induced EMT.

E-cadherin is recognised as the main marker of epithelial morphology [49], and E-cadherin expression usually decreases during EMT, while the levels of mesenchymal specific marker vimentin increase [50]. We determined vimentin and E-cadherin mRNA expression and monoclonal antibody levels correlated to the increase in EMT in the A549 and M2c macrophage co-cultures were more significant than M2a macrophage groups.

Conclusion

M2c macrophages promote EMT in lung cancer cells, according to our findings. M1 macrophages, on the other hand, reduce the proliferation and viability of A549 cancer cells and induce apoptosis in those cells. The observed inhibition of M2c-induced EMT in A549 cells exposed to bortezomib and ixazomib has provided insight into an unknown aspect of proteasome inhibition of the EMT pathway, which is the current therapeutic approach. This is the first study to show that hydrocortisone polarizes M2c macrophages, to our knowledge. Our findings suggest that in lung cancer patients taking glucocorticoid-related drugs, the M1/M2 macrophage amount in the tumor microenvironment should be investigated. Finally, polarising tumour-associated macrophages to M1 and eliminating M2a or particularly M2c macrophages, after additional investigation, might represent effective future anti-cancer therapy strategies.

Funding This study was funded by Anadolu University Scientific Research Projects (grant number 1704S095.).

Data availability All data generated or analysed during this study are included in this published article (and its supplementary information files).

Declarations

Conflict of interest Author Selin Engür-Öztürk declares that she has no conflict of interest. Author Miriş Dikmen declares that she has no conflict of interest.

Ethical approval This article does not contain any studies with human participants or animals performed by any of the authors.

References

1. Siegel RL, Miller KD, Jemal A (2019) Cancer statistics, 2019. CA A Cancer J Clin 69(1):7–34
2. Thai AA, Solomon BJ, Sequist LV, Gainor JF, Heist RS (2021) Lung cancer. Lancet 398(10299):535–554. https://doi.org/10.1016/S0140-6736(21)00312-3
3. Ben-Baruch A (2006) Inflammation-associated immune suppression in cancer: the roles played by cytokines, chemokines and additional mediators. Semin Cancer Biol 16(1):38–52
4. Sedighzadeh SS, Khoshbin AP, Razi S, Keshavarz-Fathi M, Rezaei N (2021) A narrative review of tumor-associated macrophages in lung cancer: regulation of macrophage polarization and therapeutic implications. Transl Lung Cancer Res 10(4):1889–1916
5. Sousa S, Brion R, Lintunen M, Kronqvist P, Sandholm J, Mönkkönen J, Kellokumpu-Lehtinen P, Lauttia S, Tynninen O, Joensuu H, Heymann D, Määttä JA (2015) Human breast cancer cells educate macrophages toward the M2 activation status. Breast Cancer Res 17(1):101. https://doi.org/10.1186/s13058-015-0621-0
6. Mills CD, Kincaid K, Alt JM, Heilman MJ, Hill AM (2000) M-1/M-2 macrophages and the Th1/Th2 paradigm. J Immunol 164(12):6166–6173. https://doi.org/10.4049/jimmunol.164.12.6166
7. Anderson CF, Mosser DM (2002) A novel phenotype for an activated macrophage: the type 2 activated macrophage. J Leukoc Biol 72(1):101–106. https://doi.org/10.1189/jlb.72.1.101

8. Foey AD (2014) Macrophages — Masters of Immune Activation, Suppression and Deviation. In: Duc GHT (ed) Immune Response Activation. IntechOpen, London
9. Finnin M, Hamilton JA, Moss ST (1999) Characterization of a CSF-induced proliferating subpopulation of human peripheral blood monocytes by surface marker expression and cytokine production. J Leukoc Biol 66(6):953–960. https://doi.org/10.1002/jlb.66.6.953
10. Verreck FA, de Boer T, Langenberg DM, van der Zanden L, Ottenhoff TH (2006) Phenotypic and functional profiling of human proinflammatory type-1 and anti-inflammatory type-2 macrophages in response to microbial antigens and IFN-gamma- and CD40L-mediated costimulation. J Leukoc Biol 79:285–293. https://doi.org/10.1189/jlb.0105015
11. Mosser DM, Edwards JP (2008) Exploring the full spectrum of macrophage activation. Nat Rev Immunol 8(12):958–969. https://doi.org/10.1038/nri2448
12. Martinez FO, Helming L, Gordon S (2009) Alternative activation of macrophages: an immunologic functional perspective. Annu Rev Immunol 27:451–483. https://doi.org/10.1146/annurev.immunol.021908.132532
13. Tsai MJ, Chang WA, Huang MS, Kuo PL (2014) Tumor microenvironment: a new treatment target for cancer. ISRN Biochem 2014:351959. https://doi.org/10.1155/2014/351959
14. Gao D, Vahdat LT, Wong S, Chang JC, Mittal V (2012) Microenvironmental regulation of epithelial-mesenchymal transitions in cancer. Can Res 72(19):4883–4889. https://doi.org/10.1158/0008-5472.CAN-12-1223
15. Micalizzi DS, Farabaugh SM, Ford HL (2010) Epithelial-mesenchymal transition in cancer: parallels between normal development and tumor progression. J Mammary Gland Biol Neoplasia 15(2):117–134. https://doi.org/10.1007/s10911-010-9178-9
16. Podo F, Buydens LM, Degani H, Hilhorst R, Klipp E, Gribbestad IS, Van Huffel S, van Laarhoven HW, Luts J, Monleon D, Postma GJ, Schneiderhan-Marra N, Santoro F, Wouters H, Russnes HG, Sørlie T, Tagliabue E, Børresen-Dale AL, FEMME Consortium (2010) Triple-negative breast cancer: present challenges and new perspectives. Mol Oncol 4(3):209–229. https://doi.org/10.1016/j.molonc.2010.04.006
17. Hsu YL, Chen CY, Lin IP, Tsai EM, Kuo PL, Hou MF (2012) 4-Shogaol, an active constituent of dietary ginger, inhibits metastasis of MDA-MB-231 human breast adenocarcinoma cells by decreasing the repression of NF-κB/Snail on RKIP. J Agric Food Chem 60(3):852–861. https://doi.org/10.1021/jf2052515
18. Shishodia S, Aggarwal BB (2002) Nuclear factor-kappaB activation: a question of life or death. J Biochem Mol Biol 35(1):28–40. https://doi.org/10.5483/bmbrep.2002.35.1.028
19. Fricker LD (2020) Proteasome inhibitor drugs. Annu Rev Pharmacol Toxicol 60:457–476
20. Engür S, Dikmen M, Öztürk Y (2016) Comparison of antiproliferative and apoptotic effects of a novel proteasome inhibitor MLN2238 with bortezomib on K562 chronic myeloid leukemia cells. Immunopharmacol Immunotoxicol 38(2):87–97. https://doi.org/10.3109/08923973.2015.1122616
21. Engür S, Dikmen M (2017) The evaluation of the anti-cancer activity of ixazomib on Caco2 colon solid tumor cells, comparison with bortezomib. Acta Clin Belg 72(6):391–398. https://doi.org/10.1080/17843286.2017.1302623
22. Sunwoo JB, Chen Z, Dong G, Yeh N, Crowl Bancroft C, Sausville E, Adams J, Elliott P, Van Waes C (2001) Novel proteasome inhibitor PS-341 inhibits activation of nuclear factor-kappa B, cell survival, tumor growth, and angiogenesis in squamous cell carcinoma. Clinical Cancer Res 7(5):1419–1428
23. Dikmen M, Öztürk SE, Cantürk Z, Ceylan G, Karaduman AB, Yamaç M (2020) Anticancer and antimetastatic activity of Hypomyces chrysospermus, a cosmopolitan parasite in different human cancer cells. Mol Biol Rep 47(5):3765–3778
24. Dikmen M, Canturk Z, Kaya-Tilki E, Engur S (2017) Evaluation of antiangiogenic and antimetastatic Effects of Penicillium chrysogenum Secondary Metabolites. Indian J Pharm Sci 79(1):49–57. https://doi.org/10.4172/pharmaceutical-sciences.1000200
25. Yuksel SN, Dikmen M, Canturk Z (2021) Evaluation of real-time cell proliferation, anti-inflammatory and wound healing potential of helenalin on HaCaT keratinocytes treated with lipopolysaccharide stimulated monocytes. Indian J Pharm Sci 83(2):219–229
26. Kaya-Tilki E, Engür-Öztürk S, Özarda MG, Cantürk Z, Dikmen M (2021) Investigation of the neuroprotective and neuritogenic effects of halotolerant Penicillium flavigenum-derived sorbicillin-like compounds on PC-12 Adh cells. Cytotechnology 73(6):801–813. https://doi.org/10.1007/s10616-021-00498-9
27. Mustafa AM, Caprioli G, Dikmen M, Kaya E, Maggi F, Sagratini G, Öztürk Y (2015) Evaluation of neuritogenic activity of cultivated, wild and commercial roots of Gentiana lutea L. J Func Foods 19:164–173. https://doi.org/10.1016/j.jff.2015.09.018
28. Yuan A, Hsiao YJ, Chen HY, Chen HW, Ho CC, Chen YY, Liu YC, Hong TH, Yu SL, Chen JJ, Yang PC (2015) Opposite effects of M1 and M2 macrophage subtypes on lung cancer progression. Sci Rep 5:14273. https://doi.org/10.1038/srep14273
29. Godugu C, Patel AR, Desai U, Andey T, Sams A, Singh M (2013) AlgiMatrix™ based 3D cell culture system as an in-vitro tumor model for anticancer studies. PLoS ONE 8(1):e53708. https://doi.org/10.1371/journal.pone.0053708
30. Forde PM, Kelly RJ, Brahmer JR (2014) New strategies in lung cancer: translating immunotherapy into clinical practice. Clinical Cancer Res 20(5):1067–1073. https://doi.org/10.1158/1078-0432.CCR-13-0731
31. Stein M, Keshav S, Harris N, Gordon S (1992) Interleukin 4 potently enhances murine macrophage mannose receptor activity: a marker of alternative immunologic macrophage activation. J Exp Med 176(1):287–292. https://doi.org/10.1084/jem.176.1.287
32. Varin A, Gordon S (2009) Alternative activation of macrophages: immune function and cellular biology. Immunobiology 214(7):630–641. https://doi.org/10.1016/j.imbio.2008.11.009
33. Gordon S, Martinez FO (2010) Alternative activation of macrophages: mechanism and functions. Immunity 32(5):593–604. https://doi.org/10.1016/j.immuni.2010.05.007
34. Yeung OW, Lo CM, Ling CC, Qi X, Geng W, Li CX, Ng KT, Forbes SJ, Guan XY, Poon RT, Fan ST, Man K (2015) Alternatively activated (M2) macrophages promote tumour growth and invasiveness in hepatocellular carcinoma. J Hepatol 62(3):607–616. https://doi.org/10.1016/j.jhep.2014.10.029
35. Genin M, Clement F, Fattaccioli A, Raes M, Michiels C (2015) M1 and M2 macrophages derived from THP-1 cells differentially modulate the response of cancer cells to etoposide. BMC Cancer 15:577. https://doi.org/10.1186/s12885-015-1546-9
36. Chanput W, Mes JJ, Savelkoul HF, Wichers HJ (2013) Characterization of polarized THP-1 macrophages and polarizing ability of LPS and food compounds. Food Funct 4(2):266–276. https://doi.org/10.1039/c2fo30156c
37. Huang X, Li Y, Fu M, Xin HB (2018) Polarizing macrophages in vitro. In: Rousselet G (ed) Macrophages. Springer, NY, pp 119–126
38. Dutaud D, Aubry L, Henry L, Levieux D, Hendil KB, Kuehn L, Bureau JP, Ouali A (2002) Development and evaluation of a sandwich ELISA for quantification of the 20S proteasome in human plasma. J Immunol Methods 260(1–2):183–193. https://doi.org/10.1016/s0022-1759(01)00555-5
39. Chauhan D, Tian Z, Zhou B, Kuhn D, Orlowski R, Raje N, Richardson P, Anderson KC (2011) In vitro and in vivo selective antitumor activity of a novel orally bioavailable proteasome

inhibitor MLN9708 against multiple myeloma cells. Clinical Cancer Res 17(16):5311–5321. https://doi.org/10.1158/1078-0432.CCR-11-0476
40. Wei X, Zhou P, Lin X, Lin Y, Wu S, Diao P, Xie H, Xie K, Tang P (2014) MLN2238 synergizes BH3 mimetic ABT-263 in castration-resistant prostate cancer cells by induction of NOXA. Tumour Biol 35(10):10213–10221. https://doi.org/10.1007/s13277-014-2333-y
41. Augello G, Modica M, Azzolina A, Puleio R, Cassata G, Emma MR, Di Sano C, Cusimano A, Montalto G, Cervello M (2018) Preclinical evaluation of antitumor activity of the proteasome inhibitor MLN2238 (ixazomib) in hepatocellular carcinoma cells. Cell Death Dis 9(2):28. https://doi.org/10.1038/s41419-017-0195-0
42. Van Ginderachter JA, Movahedi K, Hassanzadeh Ghassabeh G, Meerschaut S, Beschin A, Raes G, De Baetselier P (2006) Classical and alternative activation of mononuclear phagocytes: picking the best of both worlds for tumor promotion. Immunobiology 211(6–8):487–501. https://doi.org/10.1016/j.imbio.2006.06.002
43. Wang Y, Shi J, Chai K, Ying X, Zhou BP (2013) The role of snail in EMT and tumorigenesis. Curr Cancer Drug Targets 13(9):963–972. https://doi.org/10.2174/15680096113136660102
44. Dash S, Sarashetti PM, Rajashekar B, Chowdhury R, Mukherjee S (2018) TGF-β2-induced EMT is dampened by inhibition of autophagy and TNF-α treatment. Oncotarget 9(5):6433–6449
45. Suarez-Carmona M, Lesage J, Cataldo D, Gilles C (2017) EMT and inflammation: inseparable actors of cancer progression. Mol Oncol 11(7):805–823. https://doi.org/10.1002/1878-0261.12095
46. Yang Y, Luo NS, Ying R, Xie Y, Wang CJY, XQ, Gu ZJ, Mai JT, Liu WH, Wu MX, Chen ZT, Fang YB, Zhang HF, Zuo ZY, Wang JF, Chen YX, (2017) Macrophage-derived foam cells impair endothelial barrier function by inducing endothelial-mesenchymal transition via CCL-4. Int J Mol Med 40(2):558–568. https://doi.org/10.3892/ijmm.2017.3034
47. Sawa-Wejksza K, Kandefer-Szerszeń M (2018) Tumor-associated macrophages as target for antitumor therapy. Arch Immunol Ther Exp 66(2):97–111. https://doi.org/10.1007/s00005-017-0480-8
48. Huber MA, Azoitei N, Baumann B, Grünert S, Sommer A, Pehamberger H, Kraut N, Beug H, Wirth T (2004) NF-kappaB is essential for epithelial-mesenchymal transition and metastasis in a model of breast cancer progression. J Clin Investig 114(4):569–581. https://doi.org/10.1172/JCI21358
49. Tsai JH, Yang J (2013) Epithelial-mesenchymal plasticity in carcinoma metastasis. Genes Dev 27(20):2192–2206. https://doi.org/10.1101/gad.225334.113
50. Varga J, De Oliveira T, Greten FR (2014) The architect who never sleeps: tumor-induced plasticity. FEBS Lett 588(15):2422–2427. https://doi.org/10.1016/j.febslet.2014.06.019